1-1-2010

Discrete Element Simulation Validation: Impact Plate Transfer Station

Andrew Grima
University of Wollongong, agrima@uow.edu.au

Peter W. Wypych
University of Wollongong, peter_wypych@uow.edu.au

Discrete Element Simulation Validation: Impact Plate Transfer Station

A.P. Grima and P.W. Wypych

Centre for Bulk Solids and Particulate Technologies, Faculty of Engineering

University of Wollongong, Northfields Avenue, Wollongong, 2522, New South Wales, Australia

E-mail address: a.p.grima@gmail.com

Abstract

The design of conveyor transfer stations can be a complex process to ensure that reliable flow of bulk material will occur with minimal impact on infrastructure and the environment. Classical analytical methods can be used to provide a quantitative description of the flow of bulk solids through a transfer point in regards to trajectory and velocity distribution. Discrete Element Method (DEM) is a popular alternative numerical technique for modelling and visualising gross discontinuous material flow behaviour by analysing individual particle trajectories and interactions. The Discrete Element Method methodology has been well established but there is a lack of detailed validation of DEM models to experimental data and methods to calibrate DEM models to attain accurate predictions and results.

This paper presents a detailed comparative analysis between classical analytical methods and DEM to predict the flow mechanisms associated with the deformation of a bulk material impacting a flat plate. Results from DEM simulations and analytical models are compared with experimental results from a variable-geometry conveyor transfer facility to validate and evaluate the numerical methods to solve particulate flow problems. The study has focused on evaluating the ability to accurately model material discharge trajectories, the velocity of impact from the inflowing stream, the velocity of the material stream after impingement and the resultant forces on the impact plate. Methods to effectively calibrate the DEM material interaction parameters and scale parameters (e.g. particle size, solid density and particle stiffness) to reduce computational time and resources are evaluated to quantify the validity of the modelling technique against experimental results.

1 INTRODUCTION

Belt conveyor systems are a popular method for the continuous conveying of bulk solids and have been used extensively in industry over a long period of time as they have proven to be reliable and versatile for a wide range of applications and environments. The design procedures and design tools available to design and analysis belt conveyor layouts, supporting structures, drive mechanisms and control systems is widely available and extensively validated. However, one of the most undoubtedly important section(s) of a belt conveying systems is the design of equipment to load or transfer bulk material on or between belts. Often transfer stations or loading methods determine how successful and reliable a belt conveying system will be in regards to belt life, maintenance costs, down time, dust emissions, spillage, belt tracking and potential damage to the bulk material (i.e. breakage, degradation). Transfer points can unfortunately be sensitive to changes in bulk material flow characteristics which create flow problems such as material build up, wear and flooding if transfer chute assembles are not correctly designed for the anticipated bulk material properties. The lack of attention in the design and analysis of transfer points such as chute angles, ledges, cross-sectional areas of material streams, impact angles, impact forces, particle trajectories and stream velocities can lead to relentless problems which can be potentially costly and decrease the efficiency

of belt conveying systems. The ability to design a transfer point to adequately receive material from the discharge pulley and redirect the material centrally onto the receiving conveyor belt(s) with sufficient momentum to ensure that the velocity component of the material stream parallel to the receiving conveyor are similar and that any unnecessary horizontal velocity component from the material stream is removed can be a formidable task.

Analytical models are available to analysis the velocity of the material stream through transfer stations and determine the trajectory of particles. Prediction of discharge trajectories and the divergence of the material stream from the discharge pulley is important to accurately determine the location and geometry of chutes, impact plates and ledges to successfully direct the material stream. Numerous analytical methods have been developed to predict the upper and lower trajectory boundaries from the discharge pulley which vary in complexity and properties (e.g. adhesion, divergent coefficients, air drag, slip and boundary friction) that are incorporated into the models [1]. Impact plates are commonly used to redirect materials which are abrasive or consist of a lot of lump rocks which are not ideal for curved chutes (i.e. hoods). Impact plates are typically designed as a sacrificial item or have sacrificial parts but the location of the impact surfaces and the angle of impact of the material stream against the impact plate govern the acceptable life against wear [2].

The positioning of the impact plate and the surrounding confinement structures is critical for optimum performance of an impact plate type transfer station. Analytical models such as Korzen [3] analyse the complex process of cohesionless and cohesive materials impinging a vertical or inclined plate. The Korzen model describes the variation of the resultant velocity prior to impact and after impact to determine the forces exerted by the bulk material onto the impact surface. A majority of analytical methods analyse material streams in two dimensions typically along the central segment of the stream with the greatest thickness. The ability to comprehensively understand and visualise individual particle behaviour and trajectories is rather limited using analytical methods. Evaluating the flow of a bulk material to ensure that flow problems will not occur in the upper and lower sections of transfer points which use ledges (i.e. rock boxes) or novel mechanisms is difficult without using some sort of empirical method.

The discrete element method (DEM) is a numerical modelling technique which is ideal for solving engineering problems which exhibit discontinuum behaviour as the motion and interaction of each individual discrete particle or cluster of particles is explicitly modelled. Although it is a computationally intensive technique where simulation times are governed by contact detection algorithms, contact models, the size and number of particles, the size of the simulation domain and computational resources (i.e. parallel processing and memory), DEM has proven to be an optimal design tool for material handling equipment [4-7]. DEM allows complex geometries and particles to be modelled using computer-aided engineering (CAE) tools where design parameters within the DEM model are varied to improve the overall performance of material flow through equipment and potentially increase process efficiency, throughput and product quality. A considerable amount of quantitative and qualitative data can be extracted from DEM models, however, scientific and validated methodologies are required to characterise material behaviour numerically against laboratory data to warrant that DEM predictions are valid and realistic [6]. Further research is still required to explore simple and quick procedures to measure and calibrate DEM material parameters and microproperties, depending on the application of the model. Although complete validation of numerical models to analyse complex natural systems is impossible [8], this paper presents numerous techniques to calibrate the DEM model to analysis the flow of a cohesionless bulk material impinging a vertical impact plate where the DEM data is quantitatively and qualitatively compared to experimental and analytical data. Previous validation work has been conducted on a high throughput impact plate transfer by Katterfeld et al. [9] where impact forces on an impact plate and idlers on the receiving conveyor belt were measured and compared to DEM data.

2 ANALYTICAL MODELS

Rheological approaches to rationally calculate the resultant forces and velocities of bulk material impinging an impact plate provide reasonable approximations using Bernoulli's principle and applying the impulse-momentum equation to a specified control volume [10]. The Korzen method is an approach which considers the complex plastic deformation of cohesive and cohesionless bulk materials impinging a flat surface. The Korzen model incorporates Newton's laws of motion but is devised to be easily implemented in to belt conveying applications by taking into account the conveyor belt inclination angle α_b, the angle of the impact plate β and initial belt conveyor discharge conditions, such as the discharge angle α_d, discharge velocity V_d and the thickness of the material stream h_b discharging off the conveyor belt, shown in Fig. 1. When an inflowing stream of material strikes a flat surface, the formation of a pseudo static wedge of material above the main stream is possible depending on the impact angle and the friction between the bulk material and the impact plate $\mu_{p.w}$. The presence of the build-up zone introduces plastic deformation between the moving stream and the stationary zone which is a drawback in using a fluid mechanics or an Eulerian type model. Korzen's model is based on the assumption that bulk materials behave like a continuum and evaluates the material flow two-dimensionally to simplify the analysis. The lateral spreading of material and generation of secondary material streams after impingement are not specifically addressed in the Korzen model which could reduce its ability to accurately predict the particle velocity and the thickness of the stream after impingement.

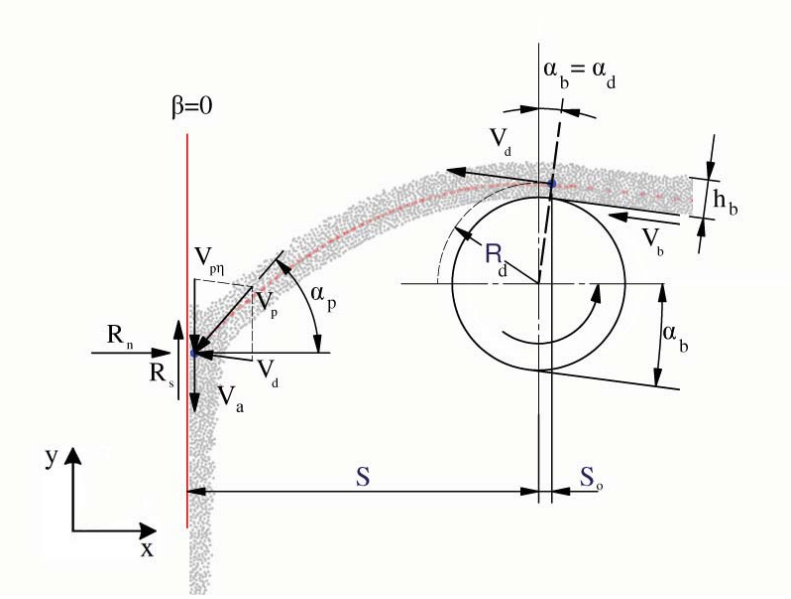

Fig. 1 Geometrical and kinematic conditions of cohesionless flow of bulk material on a flat vertical plate, adapted from [3]

The location of the impact forces is generally considered to be situated at the centroid of the load shape. Korzen assumes that the centroid of the discharging load shape is located at the centre of the material stream ($0.5h_b$). For this analysis the approach specified by the Conveyor Equipment Manufactures Association (CEMA) [11] to determine the centroid of the load shape has been investigated to compare results to experimental and DEM data. The Booth [12] method has been adopted to calculate the upper and lower trajectory limits as well as the centre of gravity of the material load shape as there is a good correlation between the experimental and DEM data using similar bulk materials and experimental rig setup [13] and has generally resulted in reasonable predictions over a wide range of industrial conditions [7].

For non-cohesive materials and for high-speed conditions where $\alpha_d = \alpha_b$ and $V_d = V_b$, the kinematic conditions of flow on an impact plate can be evaluated using Fig. 1 and the following key relations assuming that air drag is negligibly small. The velocity of bulk material when it impacts the flat surface is given by:

$$V_p = \sqrt{V_{p\eta}^2 + V_d^2 + 2V_{p\eta}V_d \cos\left(90 + \alpha_d\right)} \tag{1}$$

where

$$V_{p\eta} = \frac{g\left(s + s_0\right)}{V_d \cos\alpha_d} \tag{2}$$

Stationary flow will occur as a result of the following relation being satisfied:

$$\alpha_p + \beta > \tan^{-1}\sqrt{\mu_{p.w}} \tag{3}$$

The velocity of the material stream after impact can be estimated using an iteration procedure to converge V_a by estimating an initial cross-sectional area of the out-flowing stream A_a using the continuity equation and the following expression:

$$V_a = V_p\sqrt{\frac{A_p}{A_a}\left[\sin^2\left(\alpha_p + \beta\right) - \mu_{p.w}\cos^2\left(\alpha_p + \beta\right)\right]} \tag{4}$$

The impulse-momentum equation provides a means for calculating directly the magnitude and direction of the reaction forces exerted by bulk material striking a flat surface. Determining the relationship between the inflow velocity of the stream V_p and the initial velocity of the stream after impingement V_a allows the normal and shear reaction forces to be evaluated by:

$$R_n = \left(\rho_{bl}A_pV_p\right)V_{px} = m_sV_{px} \tag{5}$$

$$R_s = \rho_{bl}A_pV_{py}^2 - \rho_{bl}A_aV_a^2 \tag{6}$$

Eq. 6 can also be correlated to the normal reaction force R_n as:

$$R_s = R_n\mu_{p.w} \tag{7}$$

which is useful to estimate the reaction shear force R_s when V_a in Eq. 4 can not be approximated accurately.

3 IMPLEMENTATION OF DEM MODEL

The DEM is a numerical technique that computes the trajectory and rotation of each particle in a domain over very short time steps using a numerical time integration scheme. This present work is based on the soft contact approach originally proposed by Cundall and Strack [14] which is widely used. Description of the recent developments and advances in DEM can be found in Zhu et al. [15] and an overview of the vast range of applications of DEM can be found in Zhu et al. [16]. This paper focuses on modelling dry cohesionless granular particles to simplify the DEM model and enhance the ability to verify the DEM results to experimentally obtained data.

A wide variety of constitutive contact models have been proposed to date which consist of a normal and tangential stiffness model and a slip model that are ideal for modelling granular particles. Realistically modelling granular materials in many

industrial applications often requires a large quantity of particles to produce the required throughput. The linear-spring-dashpot model (LSD) [14] and the non-linear visco-elastic Hertz-Mindlin no-slip model (H-M) [17; 18] are popular models for modelling granular materials as they have the capability to model large and complex engineering systems consisting of particles of varying sizes and shapes. The DEM model of the conveyor impact plate transfer station was implemented in EDEM^{TM} [19] using the Hertz-Mindlin no-slip contact model primarily and the linear-spring-dashpot model to investigate particle flow behaviour and to better understand the particle-structure interactions.

The main difference between the LSD model and the H-M model is the relationship between the relative normal displacement at contact δ_n and the repulsive normal contact force F_n. In the LSD model the repulsive contact force is directly proportional to δ_n and the contact damping is also proportional to the relative normal contact velocity $\dot{\delta}_n$, given by:

$$F_n = k_n \delta_n + D_n \dot{\delta}_n \tag{8}$$

The repulsive normal contact force F_n in the H-M differs to the LSD model where the repulsive force is considered to be proportional the δ_n to the power of 3/2 and the contact damping is proportional to the relative normal contact velocity $\dot{\delta}_n$ to the power of 1/4, given by:

$$F_n = k_n \delta_n^{3/2} + D_n \delta_n^{1/4} \dot{\delta}_n \tag{9}$$

The normal stiffness k_n and damping coefficient D_n are determined based on material mechanical properties, such as the Young's modulus of elasticity, Poisson's ratio, solid density ρ_s and the coefficient of restitution. The equations to calculate k_n and D_n as well as further details on the tangential force calculations can be found in the EDEM user guide [20]. Depending on the contact parameters selected, the contact forces between colliding particles can differ greatly between the two contact models even though the composition of the LSD and H-M models are similar.

To realistically model particle rotational motion and account for non-spherical characteristics of real materials that can not be easily modelled such as surface asperities, sharp edges, flat surfaces and structure, a rolling resistance model is also included. The Coulomb-like rolling friction model applies a rolling friction torque to oppose the relative rotation between particles and between particles and boundaries:

$$T_R = -\mu_r \left| F_n \right| R_i \frac{\varpi_i}{\left| \varpi_i \right|} \tag{10}$$

where μ_r is the dimensionless rolling friction coefficient, R_i is the radius of particle i and ω_i is the angular velocity of particle i [21].

To maintain a stable simulation of a dynamic process, the time step Δt for the integration must be below the critical time step and is typically a small fraction of the particle contact time $t_{contact}$. The period of collision for Hertzian elastic impact is given by [22]:

$$t_{contact} \approx 2.87 \left(\frac{m^{*2}}{R^* E^* V_{rel,ij}} \right) \tag{11}$$

where $V_{rel,ij}$ is the relative velocity between two bodies and m* is the reduced mass. The critical interactions for this investigation are the collision of particles against the impact plate and hence the time step has been accordingly selected based on approximately 1/10 of the collision period using the estimated collision velocity between the particles and the impact plate.

Defining the boundaries and geometric features of the conveyor transfer in the DEM model is important to accurately model the particle-structure interactions. To accurately model and geometrically position the critical components of the conveyor transfer, such as the conveyor belts, head pulley, impact plate and chute structure, a 3D CAD model (Fig. 2) has been developed which is directly imported into EDEM where essential kinematics are applied to simulate a rotating head pulley and translating belt.

4 EXPERIMENTAL SETUP

A high-speed variable conveyor transfer research facility has been used to model impingement of bulk material onto an impact plate. The facility as shown in Fig. 2 consists of three Aerobelt^{TM} air supported belt conveyors of varying length and inclination angles which are arranged to recirculate bulk material through the transfer station to obtain steady-state conditions. Material is fed onto a conveyor from a bin through a Hogan valve which is supported by load cells that allows the mass flow rate m_s to be recorded. The belt velocity of the delivery conveyor can be easily adjusted and is manually checked using a tachometer.

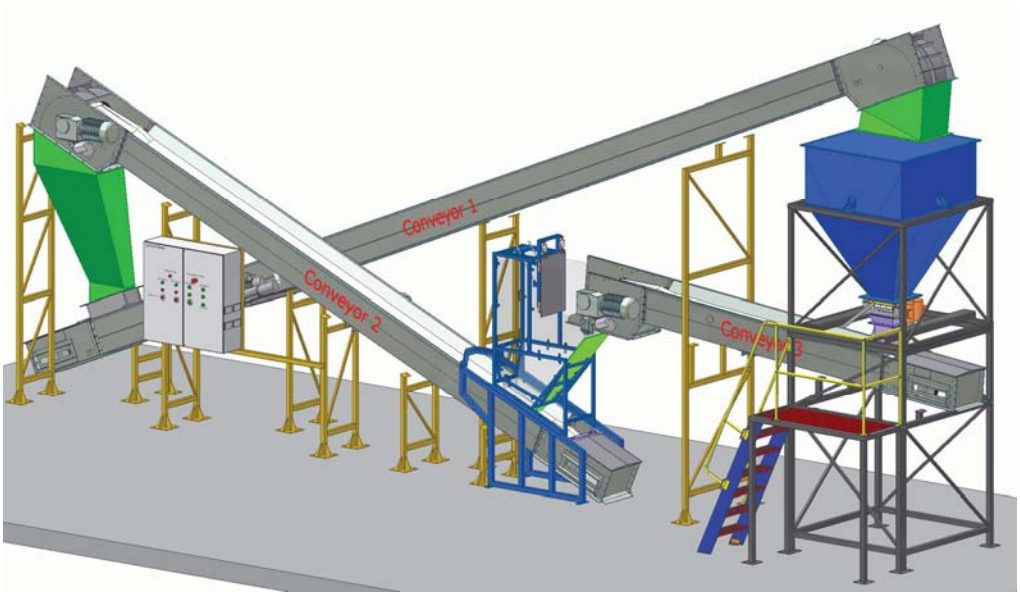

Fig. 2 Variable conveyor transfer facility with an impact plate transfer station

The impact plate transfer station which is located between two conveyors consists of a mild steel impact plate that is supported by framework with acrylic panels to contain the bulk material and allow for clear visibility of the material flow for high-speed videoing and photography during testing. Both the impact plate assembly and supporting framework assembly can be adjusted to cater for a range of belt velocities between 2 to 6m s^{-1}. Although the impact angle can be adjusted, the impact plate has been secured in a vertical position (β=0) for this investigation. Shown in Fig. 3, the impact plate is suspended by two load cells to measure the shear force and rests on four other load cells to measure the normal force on the impact plate. The impact plate is lightly restrained with a tie rod to prevent the plate from floating excessively

on the load cell buttons. Using the data from the load cells the magnitude and position of the reaction forces can be evaluated. Depending on the material discharge velocity, the distance between the impact plate and the centre of the head pulley as indicated by dimension Z in Fig. 3 is adjusted to achieve an appropriate impact angle α_p and minimise the amount of material splatter.

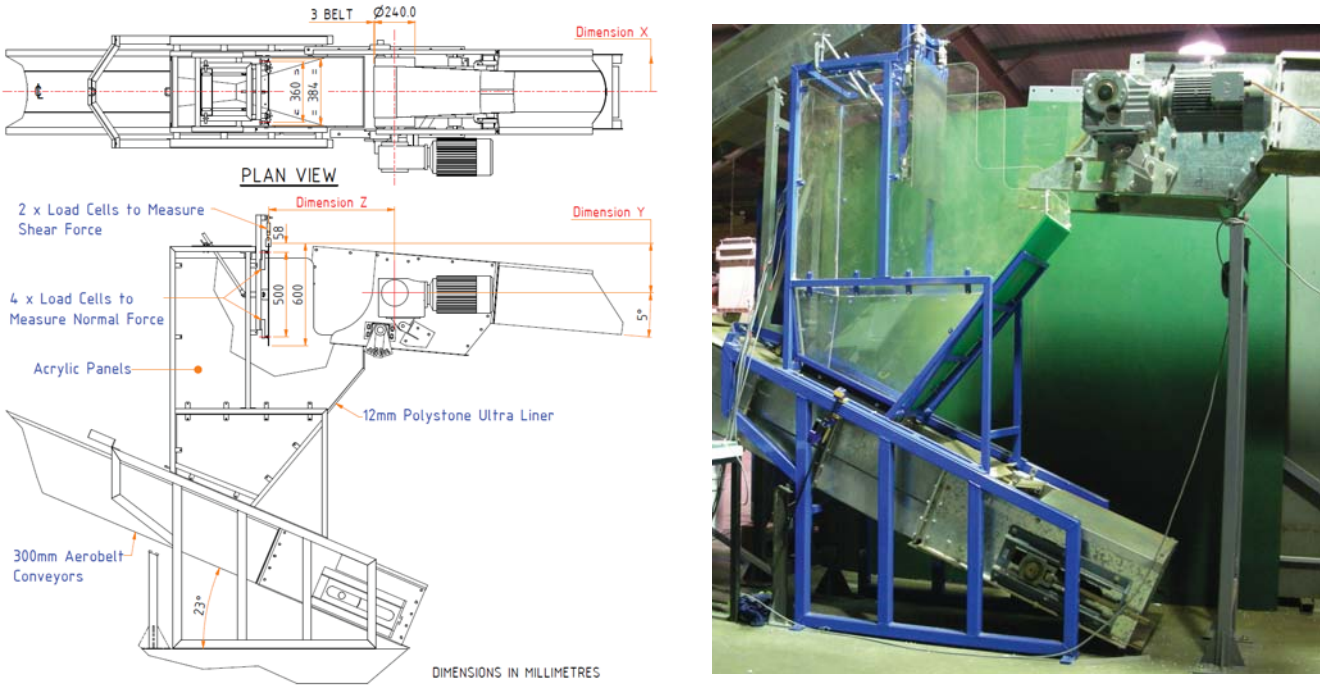

Fig. 3 Schematic (left) and photo (right) of the impact plate transfer station (left)

4.1 Experimental procedure

To examine the complex particle interactions of a stream of material striking an impact plate, a series of tests at different belt velocities V_b between 2 to 5m s^{-1} and mass flow rates m_s were conducted. Once the impact plate was in the correct position and measurements were collected for DEM and analytical models, the conveyor belt velocity was set and checked and the Hogan valve was opened to an approximate throughput. Setting a constant specified mass flow rate was difficult so the approach adopted in this work was to set the Hogan valve at approximately 20 and 40 tph and recalculate the actual mass flow rate from the data obtained to use for the DEM and analytical model input parameters. Prior to material discharge the data acquisition system was initiated to collect data from all the load cells at a frequency of 2Hz. Once steady-state flow through the transfer station occurred, data was collected for at least 10 seconds to accurately determine magnitude and location of the reaction force.

5 MATERIAL PROPERTIES AND DEM CALIBRATION OF PARAMETERS

There are only rare cases where particles are perfectly spherical and accurate measurements of the microproperties such as Young's modulus, Poisson's ratio and friction can be obtained and directly implemented. Typically, bulk materials have random particle shapes and variability in material properties as they can be heterogeneous. Direct measurement of single particle properties are not always feasible and representative. Often DEM models are simplified by using spherical particles to represent irregular particles or parameters are scaled to increase the numerical time step, hence calibration of contact models and model parameters is essential to compensate for simplifications. Linear low density polyethylene pellets shown in Fig. 4a have been selected as the test material for this investigation as the pellets are dustless and robust which improves the ability to video and photograph the material at high speed and allows for higher accuracy validation. The polyethylene

pellets are reasonably mono-sized with an average particle diameter d of 4.55mm which has been determined by averaging the measured widths of multiple particles across 3 axes. The pellets are irregular in shape but are relatively spherical where the average minor and major diameters are 3.8mm and 5.25mm, respectively. Table 1 lists the material properties for the relevant materials used in the experimental setup and DEM simulations which have been measured or approximated from available literature.

Table 1 Values of material properties

Property	Symbol	Value
Solid Density - polyethylene (kg m^{-3})	ρ_s	925
Bulk Density - polyethylene (kg m^{-3})	ρ_{bl}	535-546
Solid Density - acrylic (kg m^{-3})	ρ_s	1200
Solid Density - mild steel (kg m^{-3})	ρ_s	7800
Solid Density - conveyor belt (kg m^{-3})	ρ_s	950
Young's modulus - polyethylene (MPa)	E	250
Young's modulus - acrylic (GPa)	E	2.7
Young's modulus - mild steel (GPa)	E	182
Young's modulus - conveyor belt (MPa)	E	100
Poisson's ratio - polyethylene	ν	0.38
Poisson's ratio - acrylic	ν	0.35
Poisson's ratio - mild steel	ν	0.3
Poisson's ratio - conveyor belt	ν	0.45
Average particle diameter (mm)	d_{ave}	4.55
Average minimum particle diameter (mm)	d_{min}	3.8
Average maximum particle diameter (mm)	d_{max}	5.25

The sliding, rolling and impact behaviour of a particle and bulk material is important to characterise for analytical and numerical modelling of bulk materials. The Coulomb friction between the pellets and between the pellets and a wall material have been measured using a Jenike direct shear tester and a static friction test apparatus similar to the experimental setup shown in Li et al. [23] to compare results which are listed in Table 2. As it is difficult to measure the friction between two pellets, the coefficient of friction has been approximated by melting a quantity of pellets to form a polyethylene wall sample. The difference between the kinematic wall friction angle φ_w measured using a Jenike direct shear tester and the static wall friction angle φ_s is minor. The maximum friction angles have been selected for the DEM (μ_s) and Korzen ($\mu_{p,w}$) models as shown in Table 2. The coefficient of restitution has been measured using a high-speed camera to measure the velocity of a particle impacting a flat wall sample and rebounding off the surface. The coefficient of restitution values listed in Table 2 have been measured by taking the average result for particle impact velocities between 2 to 4m s^{-1}. The rolling behaviour of the pellets is important to characterise but direct measurement of an adequate rolling friction coefficient is not straight forward. Table 2 lists the rolling friction coefficients μ_r for particle-to-particle and particle-to-boundary interactions which have been determined with simple calibration techniques described in the following section.

Table 2 Summary of interaction parameters for polyethylene pellets used in the DEM model and analytical calculations

Material	Kinematic wall friction angle φ_w ($\tan^{-1}\varphi_w$)	Static wall friction angle φ_s ($\tan^{-1}\varphi_s$)	DEM and/or Korzen parameter $\mu_{s,}$ $\mu_{p.w}$	DEM parameter μ_r	Coefficient of Restitution (CoR)
Polyethylene (melted plate)	16.5 (0.3)	15.8 (0.28)	0.3	0.1	0.7
Acrylic	18 (0.32)	16 (0.29)	0.32	0.2	0.65
Mild steel	12.3 (0.22)	15 (0.27)	0.27	0.2	0.66
Polystone Ultra	12.3 (0.22)	11.7 (0.21)	0.22	0.1	0.7
Conveyor belt	33 (0.65)	35.1 (0.7)	0.7	0.2	0.4

Spherical representation of particles in DEM is popular as they are simple to model and efficient to detect contacts during simulations. As the polyethylene pellets are not perfectly spherical, both spherical and shaped particles have been investigated as shown in Fig. 4. The shaped particles have been created by a popular method of clustering spherical elements [24] together to create a non-spherical particle which has more realistic shearing and trajectory behaviour. Simple spherical particles which have been scaled up in diameter were also examined to quantify the accuracy of using larger spherical particles to model granular flow as a method to optimise computation time. Merely increasing the particle diameter by approximately 25 percent from 4.55mm to a marginally conservative 5.6mm reduces the number of particles required by approximately 48 percent.

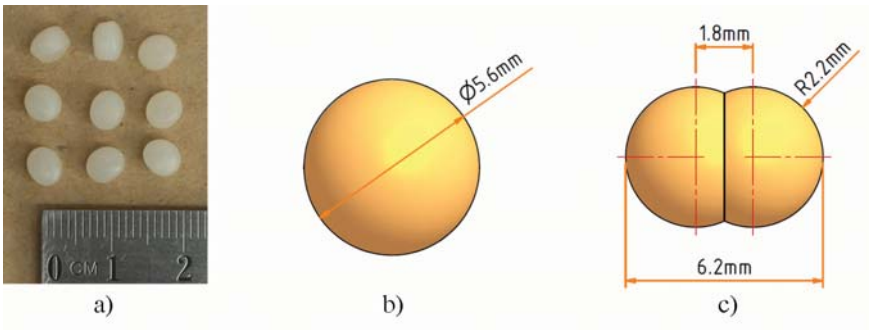

Fig. 4 Representation of the polyethylene pellets; (a) photo of polyethylene pellets, and DEM representation of the polyethylene pellets using b) a single sphere (≈ 1.25:1) and c) overlapping spheres (≈ 1:1)

A series of DEM simulations was conducted to assess the effects and computational feasibility of slightly increasing the solid density of the particles on the numerical loose-poured bulk density and the general bulk behaviour of the particles. Simultaneously, the selection of a sufficient rolling friction coefficient between particles was also examined using a newly developed swing-arm slump tester shown in Fig. 5. A small sample of bulk material is placed into the 60mm I.D. split tube which rests on a bed of bulk material in a 150mm I.D. pipe where the initial loose-poured bulk density is measured. A similar procedure is adopted in the DEM models where particles are injected into the modelled tube and allowed to settle before measurements of the bulk density are taken and compared. Once the bulk material or particles have been placed into the tube, the swing-arm opens as shown in Fig. 5 where rapid flow (i.e. similar conditions of material flow through the conveyor transfer) occurs until a conical pile is formed. By conducting several simulations altering the rolling friction coefficient and particle solid density, the optimum model parameters have been selected to achieve the closest correlation to laboratory data in regards to the loose-poured bulk density, angle of repose and shape/height of the conical pile formed. The unique ability of the swing-arm slump tester is that it is designed to primarily produce particle-to-particle interactions with negligible particle-to-boundary interactions. This is ideal to solely calibrate the particle-to-particle interactions in the DEM models.

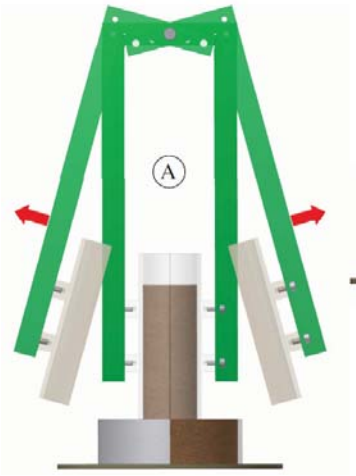

Fig. 5a Schematic of the new swing-arm slump tester

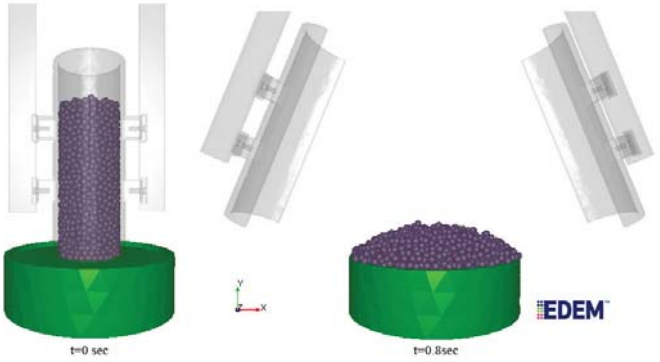

Fig. 5b DEM simulation of a slump test using the new swing-arm slump tester

The results of the simple calibration and sensitivity analysis are shown in Table 3. When the conical piles were formed in the DEM models, the angles of repose were difficult to define or were very similar using different parameters so as the height of the pile showed the greatest dependency on the rolling friction coefficient, the height of the pile and loose-poured bulk density have been evaluated for various combinations of the solid density and rolling friction coefficients in Table 3. Keeping the static friction μ_S between the particles constant, the sensitivity of the solid density on the height of pile formed is minor for both spherical and shaped particles. The influence of the rolling friction and solid density on the loose packing of particles into a cylinder is significant. A solid density of 1000 kg m^{-3} obtains a higher loose-poured bulk density which better correlates to the experimental data and is a practical method to reduce the number of particles required in a simulation and compensate for effects of scaling particles (i.e. increased voidage) and simplifying particle shapes. The smaller shaped particles pack more efficiently compared to the scaled spherical particles and achieve a higher loose-poured bulk density. Reviewing Table 3 for the most suitable rolling friction coefficient based on a solid density of 1000 kg m^{-3}, it is evident that using a shaped particle marginally requires less rolling resistance compared to spherical particles. A rolling friction coefficient of at least 0.1 for both spherical and shaped particle representation of the polyethylene pellets in the DEM model was observed to produce adequate granular flow behaviour/characteristics under rapid flow conditions and a good correlation to the loose-poured bulk density shown in Table 3. The rolling friction coefficients between the particles and wall surfaces were determined using an inclination rig to determine the required rolling resistance to prevent particles either rolling or sliding down the inclined surface prematurely. Further details on the test procedure to calibrate the rolling friction for particle-to-structure interactions can be found in Grima and Wypych [25]. The rolling resistance between the particles and the delivery conveyor belt in the DEM simulations is critical to ensure that the discharge velocity equals the belt velocity (i.e. $V_d=V_b$). If slip/rolling occurs at the discharge point in the DEM simulations, the material stream trajectories are inaccurate and the location of the impact zone on the impact plate will be lower than anticipated.

Table 3 Summary of DEM calibration of particle-to-particle rolling friction using spherical and shaped particles to represent polyethylene pellets using swing-arm slump tester where $\mu_S = 0.3$

Ideal u_r		Spherical particles d=5.6mm				Shaped particles 2 x d=4.4mm			
		Loose-poured bulk density (kg m^{-3}) ρ_{bl}		Height of pile (mm) h_p		Loose-poured bulk density (kg m^{-3}) ρ_{bl}		Height of pile (mm) h_p	
	Solid density (kg m^{-3}) ρ_s	925	1000	925	1000	925	1000	925	1000
	Exp result	535-646		27		535-646		27	
Rolling friction coefficient μ_r	0.01	523	566	18	18	546	589	21	21
	0.05	513	559	21	20	532	576	25	25
	0.1	506	549	24	26	518	561	28	27
	0.15	501	545	30	27	509	549	29	31
	0.2	497	544	31	27	502	546	29	31

6 RESULTS AND DISCUSSION

This section provides quantitative verification of the DEM and the bench-scale experiments to calibrate the DEM parameters to model the impingement of granular material onto a vertical impact plate by comparing the numerical results against experimental and analytical data. Although it cannot model discontinuous granular flow as comprehensively as the DEM, the Korzen method is suitable to verify that the experimental results are rational. The experimental data was collected and evaluated initially to determine the parameters required for the DEM and Korzen method to provide a conclusive correlation between the modelling techniques. Primarily this paper has focused on using spherical particles and the H-M contact model for the DEM analysis but the influence of the LSD contact model and various DEM input parameters has also been investigated.

Fig. 6 shows a comparison between the magnitude impact force where the velocity of the conveyor belt varies between 2 to 5m s^{-1} for low and high mass flow rates. The correlation between the experimental results and the analytical and numerical data for cohesionless material is reasonably close for experiments where the impact force is greater than 20N. As there are potential vibrations in the impact plate support system from the flow of material onto the acrylic housing and lower chutes, the fluctuations and creep in the data from the load cells are more significant when the momentum of the material is low compared to when the momentum is high. The difference between the DEM results and the experimental results is high for a belt velocity of 2m s^{-1} and typically decreases at higher discharge velocities when the bulk materials collides more directly with the impact plate ($\alpha_p \rightarrow 0°$). The error between all three techniques at a belt velocity of 5m s^{-1} and a mass flow rate of 44tph is minor. As the discharge velocity increases the drop height of the stream trajectory decreases and the impact angle α_p decreases relative to the horizontal axis as shown in Fig. 7 resulting in a greater proportion of the impact force acting normal to the impact plate.

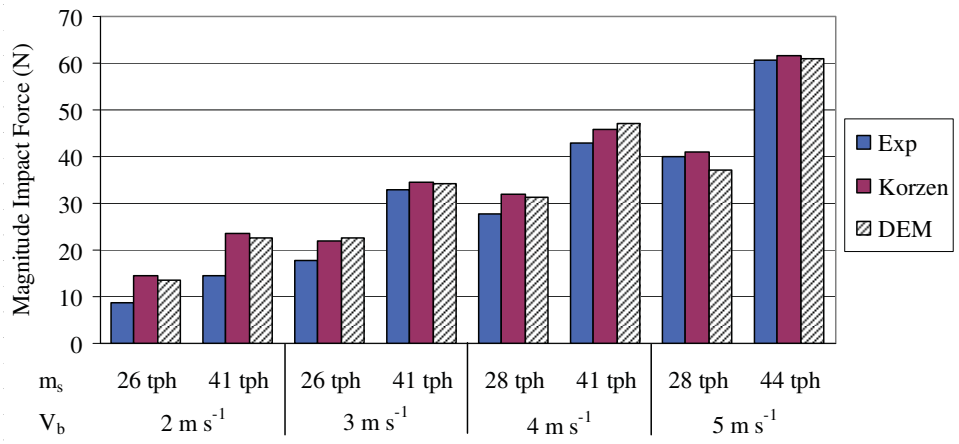

Fig. 6 Comparison of the magnitude impact force on the impact plate; DEM models: spherical particles d=5.6mm using H-M contact model

Table 4 tabulates the components of the impact force or the impact plate reaction force to compare the differences between the normal and shear forces measured or computed from each method. Comparing the experimental results to the Korzen models, the most significant deviation occurs in the calculation of the shear force R_s. It is quickly noticed that the Korzen method for cohesionless material reaches a limitation to evaluate the stream exit velocity V_a using Eq. 4. When a stationary flow does not occur as defined by Eq. 3 there is no solution to Eq. 4 due to the occurrence of negative roots which prevents the shear force to be calculated using Eq. 4. Highlighted in Tables 4 and 5, stationary flow as proposed by Korzen does not take place when $V_b \geq 4$m s^{-1} and Eq. 7 has to be implemented to calculate the shear force on the impact plate. However, the shear forces obtained using Eq. 7 in the Korzen model are considerably greater than the measured and the DEM model forces. The ratio of the shear force to the normal force (R_s/R_n) is constant in the Korzen model (i.e. $\mu_{p.w}$=0.27), however for the experimental and DEM results in Table 3, the ratio of the shear force to the normal force varies.

Table 4 Summary and comparison of impact plate reaction force results from experimental data, Korzen and DEM models; DEM models: spherical particles d=5.6mm using H-M contact model

V_b (m s^{-1})	m_s (tph)	Experimental reaction force (N)			Korzen reaction force (N)			Error between Korzen and Exp R (%)	DEM reaction force (N)			Error between DEM and Exp R (%)	Error between DEM and Korzen R (%)
		R_n	R_s	R	R_n	R_s	R		R_n	R_s	R		
2	26	7.55	4.01	8.55	14.38	2.53	14.6	70.76	13.34	3.1	13.7	60.23	-6.16
	41	13.74	4.68	14.51	23.05	4.06	23.41	61.34	21.97	5.25	22.59	55.69	-3.50
3	26	17.19	4.73	17.83	21.46	5.07	22.05	23.67	22.25	3.43	22.52	26.30	2.13
	41	32.19	6.57	32.86	33.67	7.95	34.6	5.30	33.87	5.33	34.29	4.35	-0.90
4	28	27.61	3.9	27.88	30.76	8.3*	31.86	14.28	31.07	3.53	31.28	12.20	-1.82
	41	42.49	6.88	43.05	44.36	11.98*	45.95	6.74	46.64	5.57	46.98	9.13	2.24
5	28	39.85	4.48	40.1	39.69	10.72*	41.12	2.54	36.98	3.13	37.14	-7.38	-9.68
	44	60.41	4.54	60.58	59.51	16.07*	61.64	1.75	60.62	5.02	60.84	0.43	-1.30

* Calculated using Eq. 7

To evaluate other aspects of the discharge bulk material flow off a belt conveyor and impingement with a vertical impact plate, the material stream impact velocity V_p, average velocity after impingement V_a and the location of the impact force have been analysed as shown in Table 5. The average velocity of the particles just prior to colliding with the vertical plate has been measured using a high-speed camera where particle tracking software has been used to calculate the average stream velocity. The average experimental V_p from each set of test results for different conveyor belt velocities generally

correlates well to the analytical predictions. However, the DEM models tend to under predict V_p especially at higher mass flow rates. V_p in the DEM models has been measured just as the material stream collides with the stationary flow zone or the transient material which may cause premature deceleration of the material stream before the particles accurately collide with the impact plate. The average velocity of the particles V_p after impingement in the middle of the primary material stream has been evaluated in Table 5 from experimental data to compare against the Korzen and DEM models. V_a does not fluctuate excessively and remains reasonably constant between all the experimental tests as α_p decreases with increasing V_d where greater particle deceleration occurs. V_a determined from the DEM models matches considerably well to the experimental data suggesting that the viscous damping model in the H-M contact model and the calibration method is sufficient in the numerical models. The analytical method to estimate V_a via an iteration procedure either underestimates or is unable to determine the stream velocity after impact using Eq. 4. A drawback of the Korzen model is its inability to accurately predict the flow behaviour and trajectories of a bulk solid impinging a surface especially at high velocities as the material stream proliferates in numerous directions on the impact surface making it difficult to define a control volume to calculate V_a of the central out-flowing stream based on the mass continuity equation.

Table 5 Summary and comparison of impact plate position, impact velocity V_p, stream exit velocity V_a and position of impact force location from experimental data, Booth/CEMA and DEM models; DEM models: spherical particles d=5.6mm using H-M contact model

V_b (m s^{-1})	m_s (tph)	Position of impact plate (mm)		Material discharge thickness h_b (mm)		Impact velocity V_p (m s^{-1})			Stream exit velocity V_a (m s^{-1})			Vertical distance of impact force location on impact plate from Exp (mm)		Vertical distance of impact force location on impact plate from Booth/CEMA (mm)
		Y	Z	Exp	DEM model	Exp	Korzen model	DEM model	Exp	Korzen model	DEM model	Booth/ CEMA model	DEM model	DEM model
2	26	213	500	38	40	3.03	3.04	2.84	2.35	1.4	2.13	4.5	10.3	5.8
	41			55	58	3.04		2.79	2.32	1.4	2.18	12.4	18.1	5.7
3	26	260	600	28	28	3.57	3.4	3.28	1.84	0.1	1.94	-25.8	-28.9	-3.1
	41			36	41	3.32		3.18	2.08	0.1	2	-15.9	-17.9	-2
4	28	322	760	23	24	4.39	4.21	3.77	2.15	-	2.04	-14.1	-17.9	-3.8
	41			30	33	3.94		3.54	2.8	-	2.08	-15.8	-21.1	-5.3
5	28	343	860	21	22	5.29	5.07	4.78	2.09	-	2.22	-9.5	-12.8	-3.3
	44			26	31	5.8		4.57	2.13	-	2.25	2.5	-2.8	-5.3

Table 4 shows a comparison between the locations of the impact force on the vertical impact plate determined from the experimental, analytical and numerical data. This paper only examines the discharge trajectories and locations of the impact force with respect to two spatial dimensions being Y and Z as defined in Fig. 3. Fig. 7 shows that the material trajectory as it discharges off the belt conveyor modelled using the DEM matches well to the upper and lower trajectory limits predicted from the Booth method.

The discharge of material from the feed bin onto the delivery conveyor belt was not perfectly steady and the minor fluctuations in the mass flow rate results in minor variation of the force distribution on the impact plate. Considering the experimental conditions, the error between the experimental and the Booth/CEMA and DEM results varies from 2.5mm to 28.9mm as shown in Table 5 and Fig. 7. The location of the impact force determined using the centroid of the load shape in the Booth/CEMA hybrid method matches marginally closer to the DEM models using spherical particles compared to the experimental results. The error between the Booth/CEMA predictions and the DEM models is considerably small where the DEM predictions are typically below the Booth/CEMA hybrid method. If the centre of gravity of the load shape is assumed

to be $0.5h_b$, the error between the analytical method and the DEM predictions would be slightly greater which suggests that the CEMA method is better in determining the centre of gravity of the load shape.

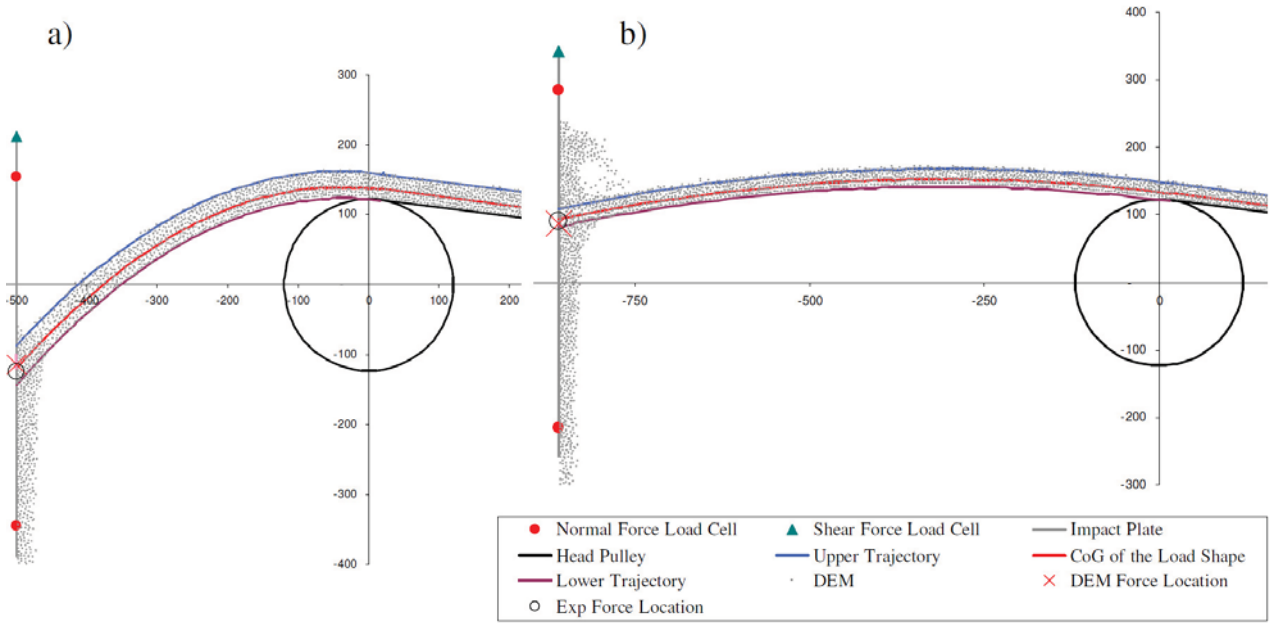

Fig. 7 Experimental, DEM and continuum results: a) $V_b = 2m\ s^{-1}$, $m_s = 26tph$ b) $V_b = 5m\ s^{-1}$, $m_s = 44tph$

The ability to visualise the trajectories of particles and the flow behaviour of particles as a bulk is a distinct advantage of the DEM compared to other analytical or numerical methods. Figs. 8 and 9 show the flow behaviour and trajectories of the particles impinging the impact plate from the laboratory experiments and DEM simulations at a low and high impact velocity. The correlation between the experimental (Fig. 8) and DEM (Fig. 9) flow patterns are generally good. The presence of the build-up zone can be distinguished in Figs. 8 and 9 especially for V_b=5m s^{-1} and m_s=44tph. Depending on the impact velocity, impact angle and mass flow rate, different flow patterns occur in relation to the quantity of material flowing around the flow-round zone predicted by the Korzen model and material flowing above the inflowing stream and laterally out of the quasi stationary zone as shown in Fig. 8. The presence of a secondary material stream is also evident in both the experimental tests and DEM simulations, especially for high mass flow rates and discharge velocities.

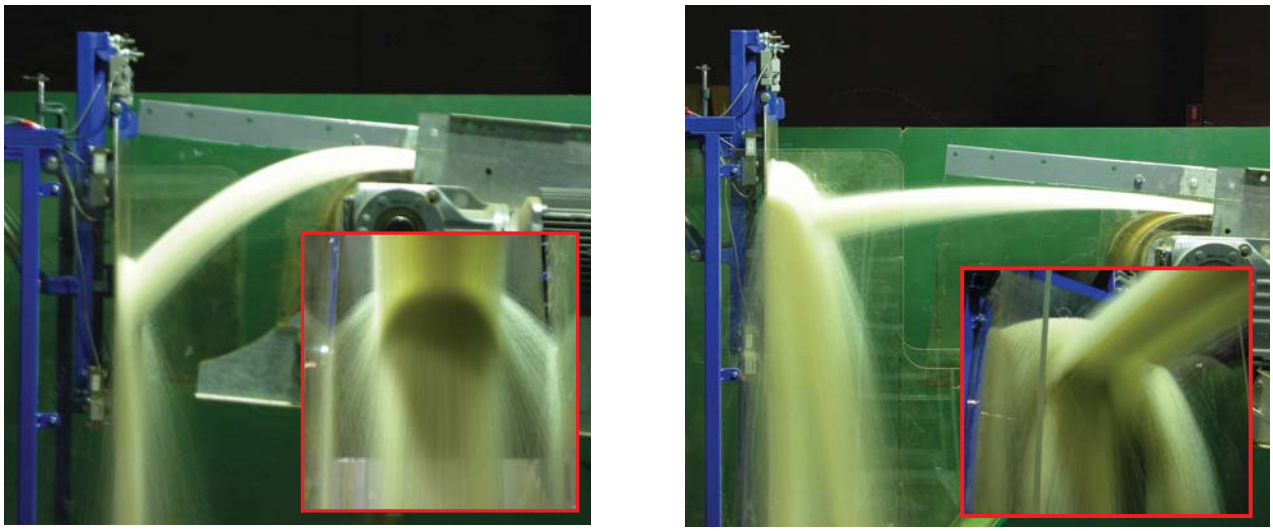

Fig. 8 Experimental snap shot of polyethylene pellets discharging from conveyor and impacting a vertical plate: $V_b = 2m\ s^{-1}$, $m_s = 26tph$ (Left), $V_b = 5m\ s^{-1}$, $m_s = 44tph$ (Right)

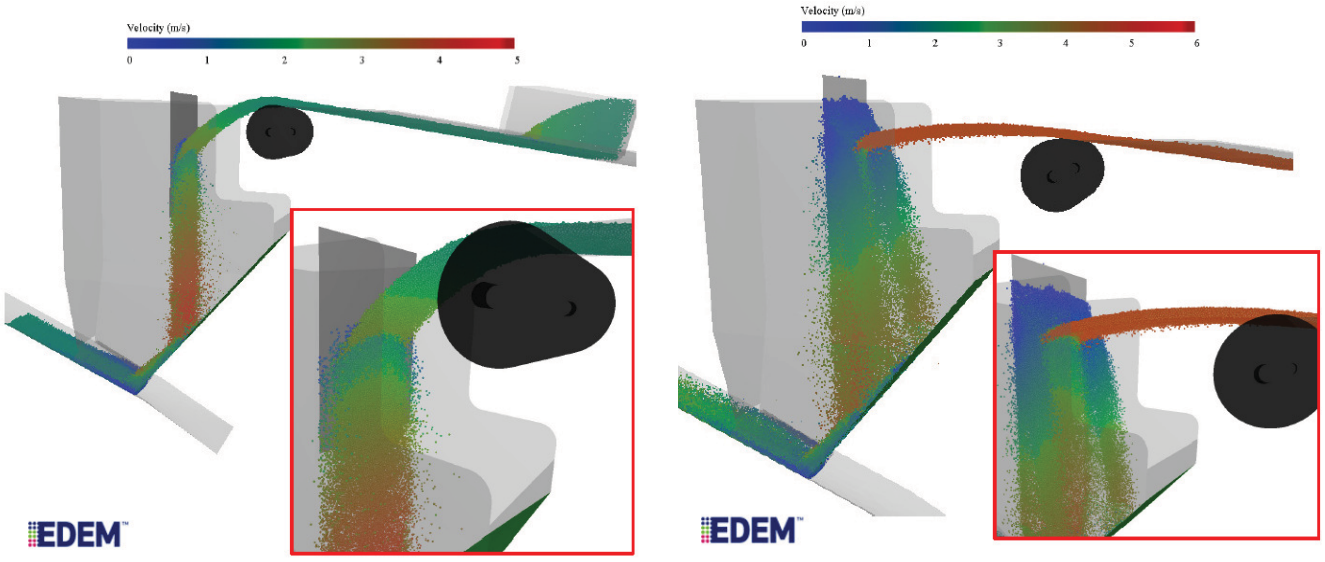

Fig. 9 DEM simulation snap shot of polyethylene pellets (spherical shape d=5.6mm) discharging from conveyor and impacting vertical plate: V_b = 2m s^{-1}, m_s = 26tph (Left), V_b= 5m s^{-1}, m_s = 44tph (Right)

6.1 Sensitivity Analysis

To investigate the sensitivity of parameters in the DEM and the selection of the constitutive contact model implemented, a series of DEM simulations was conducted to examine the deviation in the impact force. Often for large scale DEM simulations, parameters are scaled to reduce computational time but the effects of scaling DEM parameters has not been extensively studied and evaluated. Table 6 details all the parameters and contact models which were explored for the scenario where V_b= 3m s^{-1}, m_s = 41tph to determine which parameters are most sensitive and crucial for accurate modelling of granular flow.

The original LSD is a popular and appropriate contact model to model the interaction between granular materials. The variation between the impact force using the LSD and H-M contact model with similar input parameters where relevant is trivial as shown in Table 6. As the polyethylene pellets are not highly irregular in shape, the result of modelling the pellets as slightly non-spherical as shown in Fig. 4c on the computed impact force is minor compared to using simple spherical particles. Selection of a suitable numerical time step is important for numerical stability but selection of an unnecessary small time step is costly in terms of simulation time. Selection of a time step of approximately 1/10 of the collision time seems to be adequate as a time step of approximately 1/20 of the collision time does not change the computed impact force dramatically. The contact stiffness which greatly governs the critical time step and contact forces is a common parameter which is scaled down to reduce the simulation time. In this study the effects of either decreasing or increasing the shear modulus G of the particles by a factor of 10 has been investigated. The simulations in Table 6 where G was modified indicates that slightly increasing or decreasing G does not significantly alter the average total contact forces between the particles and the impact plate. Therefore, marginally reducing the contact stiffness seems to be a practical method to reduce the simulation time without excessively affecting the bulk flow of particles and particle-structure contact forces in unconfined conditions. However, applications which involve internal shearing or where the bulk elasticity is imperative, modifications to the contact stiffness may be more significant on the results obtained from a DEM model.

Scaling up particle size is a reasonable method to reduce the number of particles in a simulation and the numerical time step. This paper has mostly focused on the modelling of marginally scaled-up ($\approx 25\%$) spherical particles which have not displayed excessive errors compared to non-spherical particles in relation to the impact force but have shown some differences in the loose packing of particles as revealed in Table 3. The result of scaling up the diameter of the spherical particles by a factor of approximately 2 and 3 has been explored in Table 6. The magnitude of the impact force determined in the DEM simulations using 9mm and 13.6mm diameter particles is not drastically different from the results obtained using 5.6mm diameter particles listed in Table 4. When the particle diameter is increased without scaling other parameters, such as m_s or the scale of the geometry, the number of particles in the model can decrease rapidly depending on the degree of scale-up. As the number of particles decreases, the number of potential contacts between the particles and the impact plate decreases and varies between each time step. The weight force of each particle increases and the resultant force on the impact plate deviates greatly as the particle diameter is increased which reduces the resolution and distribution of the force and pressure on surfaces. If the distribution of the contact force on a surface is of interest (e.g wear analysis), increasing the particle size will limit the quality of data for particle-structure interactions.

Table 6 Investigation of influence of contact model, particle shape representation, time step Δt and shear modulus G on impact plate reaction force results

V_b (m s^{-1})	m_s (tph)	Contact Model	Particle shape representation	Δt (s) x 10^{-6}	Notes	DEM reaction force (N)			Error between DEM and Exp R (%)	Error between DEM and Korzen R (%)	Error between DEM and equivalent DEM model in Table 4 (%)
						R_n	R_s	R			
3	41	LSD	Spherical d=5.6mm	9.37	-	33.29	5.18	33.7	2.56	-2.60	-1.72
		H-M	Shaped d=4.4mm x 2	7.36	-	32.95	5.42	33.4	1.64	-3.47	-2.60
		H-M	Shaped d=5.6mm x 2	9.37	d increased	33.01	5.7	33.5	1.95	-3.18	-2.30
		H-M	Spherical d=5.6mm	4.67	reduced Δt	34.96	5.7	35.43	7.82	2.40	3.32
		H-M	Spherical d=5.6mm	19.8	0.1G	34.11	5.18	34.5	4.99	-0.29	0.61
		H-M	Spherical d=5.6mm	2.96	10G	33.34	5.35	33.77	2.77	-2.40	-1.52
		H-M	Spherical d=9mm	15.1	d increased	36.2	5.89	36.69	11.66	6.04	7.00
		H-M	Spherical d=13.6mm	22.4	d increased	32.62	4.77	33.05	0.58	-4.48	-3.62

7 CONCLUSIONS

This paper has explored analytical and DEM modelling techniques to understand the complex processes of the flow of granular material through a belt conveyor transfer station with an impact plate. DEM has proven to be a superior technique to model and bulk material flow compared to basic analytical techniques where large quantities of data can be obtained between particle-to-boundary contacts which can be used to improve the design and life of equipment. Methods to calibrate the DEM models to visualise and predict the trajectory of the bulk material through a transfer station and the forces of the material flow exerted onto structures have been validated against experimental and analytical data. The techniques used to measure or calibrate the DEM input parameters have revealed to be satisfactory to achieve realistic quantitative and qualitative results. In general a good correlation between DEM and experimental data was observed both qualitatively and quantitatively, however further research is still required to develop efficient and validated techniques to calibrate DEM models for large scale industrial applications.

Acknowledgements

The authors gratefully acknowledge the technical support from Leap Australia and DEM Solutions for the software package EDEM. A.P. Grima is grateful to Technological Resources Pty. Ltd. (subsidiary of Rio Tinto Ltd.) for the financial support (scholarship) for the present work. The authors also thank David Leslie (undergraduate student) for his hard work in the design and manufacture of the impact plate transfer station.

References

[1] D. B. Hastie & P. W. Wypych, The Prediction of Conveyor Trajectories – A Review, Australian Bulk Handling Review, Vol. 12, No. 2, 2007, pp. 56-65.

[2] O. J. Scott & P. R. Choules, The use of impact plates in conveyor transfers, Tribology International, Vol. 26, No. 5, 1993, pp. 353-59.

[3] Z. Korzen, Dynamics of bulks solids flow on impact plates of belt conveyor systems, Bulk Solids Handling, Vol. 8, No. 6, 1988, pp. 689-97.

[4] F. Kessler & M. Prenner, DEM – Simulation of Conveyor Transfer Chutes, FME Transactions, Vol. 37, No. 4, 2009, pp. 185-92.

[5] A. Katterfeld, T. Gröger, M. Hachmann & G. Becker, Usage of DEM Simulations for the Development of a New Chute Design in Underground Mining, in Proceedings of the 6th International Conference for Conveying and Handling of Particulate Solids (CHoPS), Brisbane, Queensland, Australia, 3-7 August, 2009, Proceedings on USB, pp. 90-95.

[6] P. W. Cleary, Industrial particle flow modelling using discrete element method, Engineering Computations, Vol. 26, No. 6, 2009, pp. 698-743.

[7] D. J. Kruse, Chute Designs and Trajectories using the Discrete Element Method, in Proceedings of BELTCON 15, Boksburg, Republic of South Africa, 2-3 September, 2009.

[8] N. Oreskes, K. Shrader-Frechette & K. Belitz, Verification, Validation, and Confirmation of Numerical Models in the Earth Sciences, Science, Vol. 263, No. 5147, 1994, pp. 641-46.

[9] A. Katterfeld, T. Gröger & A. Minkin, Discrete Element Simulation of Transfer Stations and their Verification, in Proceedings of the 9th International Conference Bulk Materials Storage, Handling & Transportation, Newcastle, NSW, Australia, 9th October, 2007, Proceeding on USB.

[10] K. W. Lonie, The Design of Conveyor Transfer Chutes, Third International Conference on Bulk Materials and Transportation, Newcastle, Australia, 27-29 June,1989.

[11] CEMA, Belt Conveyors for Bulk Materials, 6th Ed, 2nd Print, Florida, USA, Conveyor Equipment Manufactures Association, 2007.

[12] E. P. O. Booth, Trajectories from Conveyors - Method of Calculating them Corrected, Engineering and Mining Journal, Vol. 135, No. 12, 1934, pp. 552-54.

[13] D. B. Hastie & P. W. Wypych, Evaluation of Belt Conveyor Trajectories, in Proceedings of the 6th International Conference for Conveying and Handling of Particulate Solids (CHoPS), Brisbane, Queensland, Australia, 3-7 August, 2009, Proceedings on USB, pp. 299-305.

[14] P. A. Cundall & O. D. L. Strack, A discrete numerical model for granular assemblies, Géotechnique, Vol. 29, No. 1, 1979, pp. 47-65.

[15] H. P. Zhu, Z. Y. Zhou, R. Y. Yang & A. B. Yu, Discrete particle simulation of particulate systems: Theoretical developments, Chemical Engineering Science, Vol. 62, No. 13, 2007, pp. 3378-96.

[16] H. P. Zhu, Z. Y. Zhou, R. Y. Yang & A. B. Yu, Discrete particle simulation of particulate systems: A review of major applications and findings, Chemical Engineering Science, Vol. 63, No. 23, 2008, pp. 5728-70.

[17] Y. Tsuji, T. Tanaka & T. Ishida, Lagrangian numerical simulation of plug flow of cohesionless particles in a horizontal pipe, Powder Technology, Vol. 71, No. 3, 1992, pp. 239-50.

[18] A. O. Raji & J. F. Favier, Model for the deformation in agricultural and food particulate materials under bulk compressive loading using discrete element method. I: Theory, model development and validation, Journal of Food Engineering, Vol. 64, No. 3, 2004, pp. 359-71.

[19] DEM Solutions, EDEM v2.2, Edinburgh, UK, DEM Solutions Ltd, 2009.

[20] DEM Solutions, EDEM v2.2 User Guide, Edinburgh, UK, DEM Solutions Ltd, 2009.

[21] Y. C. Zhou, B. D. Wright, R. Y. Yang, B. H. Xu & A. B. Yu, Rolling friction in the dynamic simulation of sandpile formation, Physica A: Statistical Mechanics and its Applications, Vol. 269, No. 2-4, 1999, pp. 536-53.

[22] F. Li, J. Pan & C. Sinka, Contact laws between solid particles, Journal of the Mechanics and Physics of Solids, Vol. 57, No. 8, 2009, pp. 1194-208.

[23] Y. Li, Y. Xu & C. Thornton, A comparison of discrete element simulations and experiments for 'sandpiles' composed of spherical particles, Powder Technology, Vol. 160, No. 3, 2005, pp. 219-28.

[24] J. F. Favier, M. H. Abbaspour-Fard, M. Kremmer & A. O. Raji, Shape representation of axi-symmetrical, non-spherical particles in discrete element simulation using multi-element model particles, Engineering Computations, Vol. 16, No. 4, 1999, pp. 467-80.

[25] A. Grima & P. Wypych (2010), "Discrete element simulation of a conveyor impact-plate transfer: calibration, validation and scale-up", *Australian Bulk Handling Review*. Vol. 15, No. 3, 2010, pp. 64-72.